Int. J. Heat Mass Transfer. Vol. 16, pp. 591–609. Pergamon Press 1973. Printed in Great Britain

HEAT TRANSFER FOR TURBULENT FLOW WITH SUCTION IN A POROUS TUBE

J. K. AGGARWAL*
and
M. A. HOLLINGSWORTH
Department of Mechanical Engineering, University of Bristol, Bristol, England

(*Received* 21 *March* 1972 *and in revised form* 31 *July* 1972)

Abstract—Measurements of the axial surface temperature distribution have been obtained on a porous tube carrying a flow of air and subjected to uniform electrical heating. Hydrodynamically fully-developed turbulent flow existed at the tube entrance and mass extraction through its wall was uniform. The local bulk temperature of the mainstream has been evaluated with the aid of the energy equation. The experiments covered an inlet Reynolds number range of about 10^4–10^5 with a ratio of the transverse velocity at the wall to the mean axial velocity at inlet from zero to about 0·012 (i.e. from no-suction to 100 per cent suction). The radial distribution of temperature measured in the exit plane of the tube indicates that the form of the temperature profile is markedly influenced by suction, becoming steeper near the wall and flatter near the axis of the tube. Local as well as average values of the Nusselt number with suction have been computed and are presented in graphical form. At a fixed inlet Reynolds number both these values increased substantially with suction and decreased with x/D, although the *local* values relative to their no-suction counterparts increased along the tube. An empirical correlation for the average Nusselt number with suction is also presented. To describe the rate of supply of heat to the air remaining in the tube, as opposed to the total supply of heat which includes the heat supplied to the sucked air before it enters the porous wall, an 'apparent' Nusselt number has been evolved and both the local and average apparent Nusselt numbers decreased with increasing suction and x/D.

NOMENCLATURE

A, constant defined by equation (14);
a, exponent in equation (30);
B, constant defined by equation (22);
b, exponent in equation (30);
c_p, specific heat at constant pressure;
D, inside diameter of the porous tube;
h, heat transfer coefficient defined by equation (3);
h_a, apparent heat transfer coefficient with suction defined by equation (6);
$\bar{h}_a$, average apparent heat transfer coefficient with suction defined by equation (10);
h_e, effective heat transfer coefficient with suction defined by equation (5);
h_i, volumetric interstitial heat transfer coefficient;
k, thermal conductivity of air;
k_p, thermal conductivity of the porous material;
L, length of the porous tube;
m, axial mass flow rate;
N, function of x/D and β_1 in equation (31);
n, exponent in equation (30);
Nu_D, Nusselt number ($= hD/k$);
$\overline{Nu_D}$, average Nusselt number defined by equation (23);
Nu_{Da}, apparent Nusselt number with suction ($= h_aD/k$);
$\overline{Nu_{Da}}$, average apparent Nusselt number with suction ($= \bar{h}_aD/k$);
P, function of x/D and β_1 in equation (29);
p, exponent in equation (29);
Pr, Prandtl number;

* Now at the Department of Engineering Science, University of Oxford, Parks Road, Oxford, England.

Q, sum of enthalpy rises of the mainstream and the sucked air;
Q_a, average apparent heat transfer rate to the mainstream defined by equation (10);
Q_i, electrical power input to the tube;
Q_s, total heat supplied to the sucked air within the porous wall;
q, local rate of heat transfer to the air per unit x/D;
q_a, local rate of apparent heat transfer with suction, per unit x/D, defined by equation (6);
q_e, local rate of effective heat transfer with suction, per unit x/D, defined by equation (4);
q_g, rate of heat generation per unit volume;
q_L, local rate of heat loss per unit x/D;
q_m, local rate of heat transfer to the mainstream per unit x/D;
q_s, local rate of interstitial heat transfer, per unit x/D, defined by equations (19) and (20);
Re_D, Reynolds number;
r, radial distance from the tube axis;
t, temperature;
t_a, ambient temperature;
t_b, bulk temperature of the mainstream;
t_i, measured air temperature at the inner surface of the Sindanyo flange;
t_s, temperature of the sucked air;
$\overline{t_s}$, average temperature of the sucked air defined by equation (13);
t_{sw}, temperature of the sucked air at entry to the wall of the porous tube;
t_w, temperature of the inner surface of the porous tube;
t_{out}, temperature of the outer surface of the porous tube;
$\overline{\Delta t}$, arithmetic mean temperature difference defined by equation (11);
x, axial distance from entry of porous tube;
x^+, non-dimensional axial distance ($= x/D$);
w, thickness of the wall of the porous tube;
α, fractional mass extraction parameter;
β, suction coefficient (ratio of the radial velocity at the inner surface of the porous tube to the local bulk velocity of the mainstream).

Subscripts

0, quantity under no suction conditions;
1, at inlet to porous tube;
2, at outlet from porous tube;
c, corresponding to constant property;
fd, corresponding to fully-developed flow.

1. INTRODUCTION

AGGARWAL *et al.* [1] have recently determined experimentally the friction factors for the flow of air in a tube subjected to surface suction. These results are of relevance to the cooling of those parts of the gas turbine which are subjected to the highest gas temperature. The turbine entry temperature, notably in aircraft applications, has progressively risen over the years due to continuing pressure to design smaller and lighter engines producing greater thrust with improved specific fuel consumption. Hitherto, conventional air-cooling techniques, such as convective and film cooling, have sufficed to maintain the metal temperature at an acceptable level. In vectored thrust engines a short period of very high turbine entry temperature occurs at take-off, and under such circumstances a strictly limited amount of water injection comes to the rescue. For most aero-engine applications, however, air still remains the most logical coolant. Nevertheless, the expenditure involved in using ever-increasing amounts of cooling air to achieve greater cooling effectiveness follows a law of diminishing returns. Clearly there is a need for future engines to have a more efficient form of cooling, and the use of permeable materials for this purpose seems to be extremely promising. Bayley and Turner [2] have recently suggested that transpiration cooling represents the ultimate in air cooling of gas turbine components. This follows their detailed studies [3, 4] of the heat transfer performance

of a cascade of porous blades. In their work upon porous blades, Bayley and Turner were principally interested in the blade outer surface and interstitial heat transfer coefficients rather than the heat transfer coefficient between the porous material and the cooling air travelling up the spanwise passages of the blade. This latter coefficient was initially expected to influence the overall heat transfer performance only slightly, but measurements of the surface and air temperatures within these passages suggested that this coefficient was substantially greater than that pertaining to fully developed flow at the corresponding local Reynolds number, and more evidence to support these findings is given by Edwards [5, 6]. It was the object of the investigation described herein to establish more well-defined values for this coefficient over a large range of suction and using turbulent flow. Many different cross-sections of spanwise passage may be used in porous blades and the tests were therefore restricted to the most general form of passage—one of circular cross-section. The results may thus be of use also to designers in other fields of engineering.

The only known investigation of heat transfer in a circular tube with surface suction has been carried out by Kinney and Sparrow [7] who recently made an analytical study for turbulent flow, invoking the Prandtl mixing length concept to describe turbulence and postulating that the velocity profiles are locally self-similar. The latter assumption may be good enough at low suction rates, but certainly at high suction rates such as those used in the present experiments, it cannot be justified [1]. They also assumed that the temperature profiles are locally self-similar. Kinney and Sparrow found that the temperature profiles became flatter in the region of the core and steeper in the region of the wall, the latter change giving rise to an increase in the Nusselt number with suction. This is in agreement with the present findings, although due to the assumption of local similarity the effect of changing x/D could not be accounted for in Kinney and Sparrow's analysis.

In the present investigation, air at ambient temperature was passed through a porous stainless steel tube of length to diameter ratio of 20·8. The tube was heated electrically by passing alternating current through it. In order to simplify the conditions, the flow at entry was made hydrodynamically fully-developed and the suction rate was made uniform along the tube. The range of inlet Reynolds number covered was from 10000 to 100000. Keeping the inlet Reynolds number fixed, the fractional mass extraction parameter, α, was varied in steps of 0·1 from zero to unity. Measurements were made of the axial distribution of the temperature of the outer surface of the tube, the sucked air temperature and the voltage along the tube, the entry and exit mass flows and bulk temperatures of the air and the electric power supplied. Profiles of the air temperature at the inlet and outlet of the tube were also measured. These data were processed in accordance with the methods outlined in section 4 to yield Nusselt numbers with suction.

2. SOME BASIC CONSIDERATIONS

When a hydrodynamically fully-developed flow of a single phase Newtonian fluid enters a smooth, straight, constant-area, circular, impervious tube subjected to uniform heat flux then, under idealized conditions, the temperature profile deviates from the initially flat form and eventually acquires a fully-developed shape. By idealized conditions is meant the following.

1. There is no radiation or free convection.
2. There is negligible heat generation (i.e. viscous dissipation and heat of reaction) within the fluid.
3. The fluid properties affecting heat transfer are constant.

At the tube entrance, the Nusselt number is theoretically infinite due to the sudden application of heat flux at $x/D = 0$; it decreases along the tube until it finally attains a constant value determined by the Reynolds number and the Prandtl number pertaining to the flow. At this

point in the tube, the temperature profile becomes fully-developed. The thermal entrance length (defined as the tube length necessary for the local Nusselt number to diminish to a value 5 per cent greater than the corresponding fully developed value), which is also dependent upon the Reynolds number and the Prandtl number, is 10 tube diameters for air in the Reynolds number range of 10^4–10^5 [8].

When suction is applied at the wall the Nusselt number is still infinite at $x/D = 0$ (although in practice one obtains a finite value) and decreases along the tube, but it is not to be expected, however long the porous section may be, that a fully developed temperature profile can be achieved and it becomes essentially an entrance length problem. Thus one would expect to be able to correlate heat transfer data by a relation of the form

$$Nu_D = Nu_D(Re_D, Pr, x/D, \beta) \qquad (1)$$

where β is a suction parameter, defined as the ratio of the radial velocity at the wall to the local mean axial velocity. Clearly, the above relation would be modified to allow for the variation in the surface structure of the porous tube and to include the effect of surface roughness. The present results can therefore only be applied with confidence to a tube having a surface structure and roughness similar to the one tested.

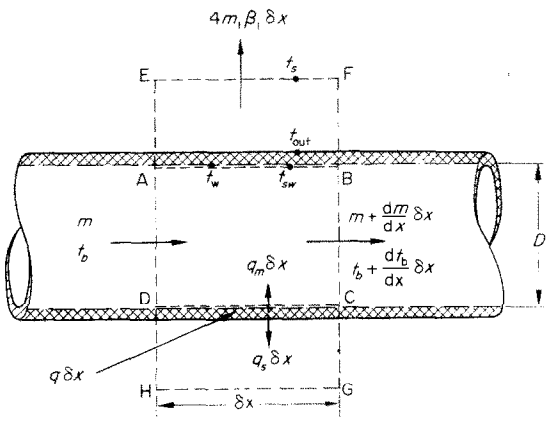

FIG. 1. Control volume for energy balance.

The heat transfer coefficient appearing in equation (1) must be defined in the context of flow with suction. Consider the energy balance in a control volume ABCD (Fig. 1) of the fluid within the porous tube, subjected to uniform wall suction. It can be shown that in the limit, as $\delta x \to 0$, the following equation applies at any x-section.

$$q_m - (4m_1\beta_1)c_p t_{sw} = \frac{d}{dx^+}(mc_p t_b) \qquad (2)$$

where subscript 1 refers to conditions at entry to the porous tube and

q_m = actual heat transfer rate from the inner surface of the porous tube to the mainstream, per unit x/D ($x^+ \equiv x/D$),
$4m_1\beta_1$ = mass flow rate of the sucked air per unit x/D,
t_{sw} = temperature of the sucked air at entry to the wall of the porous tube,
m = axial mass flow rate,
t_b = bulk temperature of the mainstream air.

A heat transfer coefficient with suction, h, may be defined by the equation

$$q_m = h\pi D^2(t_w - t_b) \qquad (3)$$

where t_w = temperature of the inner surface of the porous tube.

This heat transfer coefficient, which relates to the total supply of heat from the inner surface, cannot be computed from experimental data, however, because it appears impossible to measure the temperature at which the sucked air enters the porous surface, a knowledge of t_{sw} being required for the calculation of q_m from equation (2). Nevertheless, a value for h can be established if the interstitial heat transfer coefficient, h_i, relating to the heat transfer occurring in the wall, is known. This has been done using the data for h_i from Bayley and Turner [9], the method of calculation being outlined in section 4.

Out of the total heat supplied to the mainstream, a part is sucked back with the flow through the wall; therefore a heat transfer co-

efficient based on the remaining enthalpy will perhaps be more useful to the designer. The two terms on the left hand side of equation (2) can be lumped together and the composite quantity called 'effective heat transfer rate with suction' per unit x/D, q_e, to the mainstream. Thus q_e represents the rate of rise of enthalpy of the mainstream along the tube,

$$q_e = q_m - (4m_1\beta_1)c_p t_{sw} = \frac{\mathrm{d}}{\mathrm{d}x^+}(mc_p t_b). \quad (4)$$

The corresponding 'effective heat transfer coefficient with suction' can now be defined by the equation

$$q_e = h_e \pi D^2 (t_w - t_b). \quad (5)$$

The value of h_e can be computed from experimental data because the extreme right hand side of equation (4) is known. However, it can easily be demonstrated that this form of the heat transfer coefficient results in values of h_e which are open to a number of objections. The effective heat transfer coefficient

1. becomes negative under certain conditions of flow and temperature;
2. is strongly influenced by the temperature difference $(t_w - t_b)$ and in the extreme case when $(t_w - t_b) \to$ zero (i.e. isothermal flow), $h_e \to -\infty$;
3. depends upon whether the bulk temperature of air used in the computation is taken as absolute or relative.

This clearly leads to great complication when quoting values for h_e and, although perfectly valid, negative values of h_e have an irrational appearance. It is desirable therefore to modify the above definition of heat transfer coefficient and the most straightforward modification is to define it in terms of the rate of rise of the bulk temperature of air along the tube viz:

$$q_a = mc_p \frac{\mathrm{d}t_b}{\mathrm{d}x^+} = h_a \pi D^2 (t_w - t_b). \quad (6)$$

Since q_a does not represent the actual heat transfer rate to the main stream from the inner surface of the porous tube, h_a will be called the 'apparent heat transfer coefficient with suction'. It can easily be shown that such a definition resolves all the difficulties associated with the effective heat transfer coefficient mentioned earlier.

Having defined the apparent heat transfer coefficient in this way, it is important to establish independent, non-dimensional, groups upon which the apparent Nusselt number with suction would depend. A relationship between the actual and the apparent Nusselt numbers can be derived in the following manner. Taking c_p as constant, introduction of definition (6) into equation (2) gives, after some re-arrangement

$$q_a = q_m - (4m_1\beta_1)c_p(t_{sw} - t_b). \quad (7)$$

In terms of Nusselt numbers, equation (7) can be reduced to give

$$Nu_{Da} = Nu_D - \beta \frac{(t_{sw} - t_b)}{(t_w - t_b)} PrRe_D \quad (8)$$

since $\beta = \beta_1/(1 - 4\beta_1 x^+)$,

$$Re_D = Re_{D1}/(1 - 4\beta_1 x^+) \quad (9)$$

and

$$Re_{D1} = 4m_1/\pi\mu D.$$

It is quite clear that for a given value of Nu_D, Re_D, Pr, β and $(t_w - t_b)$, $(t_{sw} - t_b)$ will be unique, in which case equation (8) demonstrates that the apparent Nusselt number, Nu_{Da}, will depend upon the usual similarity parameters. Under no-suction conditions the apparent Nusselt number reverts to the actual Nusselt number.

An average apparent heat transfer rate to the mainstream with suction, up to a given location in the tube, will be defined as the product of the entry mass flow, the specific heat, and the rise in bulk temperature of air up to that location, namely

$$Q_a = m_1 c_p (t_b - t_{b1})$$

and the corresponding average apparent heat transfer coefficient with suction by the equation

$$\frac{Q_a}{x^+} = \frac{m_1 c_p (t_b - t_{b1})}{x^+} = \bar{h}_a \pi D^2 \overline{\Delta t} \quad (10)$$

where $\overline{\Delta t}$ is the arithmetic mean temperature difference given by

$$\overline{\Delta t} = \tfrac{1}{2}[(t_{w1} - t_{b1}) + (t_w - t_b)]. \quad (11)$$

Since the mainstream mass flow varies along the tube, the log-mean-temperature difference is clearly inapplicable.

3. APPARATUS AND INSTRUMENTATION

3.1 *General arrangement*

A schematic representation of the apparatus is given in Fig. 2. The air supply, which was at about 7 bar and room temperature, passed through filters, which removed oil, water and particulate matter greater than about 1 μm dia., before it entered a pressure regulator. This regulator was the primary control for the flow entering the porous tube. Between the regulator and the porous tube an orifice plate meter was installed. The flow into the porous tube and its distribution between sucked air (i.e. air passing through the wall of the tube) and mainstream air (air passing along the tube) was further controlled by valves located near the outlet points of the two flows, both of which finally discharged to atmosphere via float-type flow meters.

3.2 *The test section*

A Vokes 'Poroloy-T' stainless steel porous tube of 17·77 mm nominal internal diameter, 0·63 mm wall thickness, 30 per cent average porosity and 5 μm nominal pore size was used. Its effective length was 370 mm, giving an L/D of 20·8. This tubing is made by the Bendix Aviation Corporation of the U.S.A. by precision winding 30 layers of fine flattened wire around a mandrel and sintering it in a furnace, thus bonding the crossing wires at each point of contact, giving the surface shown magnified in Fig. 3. The tube dimensions are maintained very accurately over its complete length, but the local porosity was found to vary by up to about 40 per cent. A thin walled tube was chosen so that the heat supplied to the sucked air within the wall would be small compared with that lost from the inner surface to the

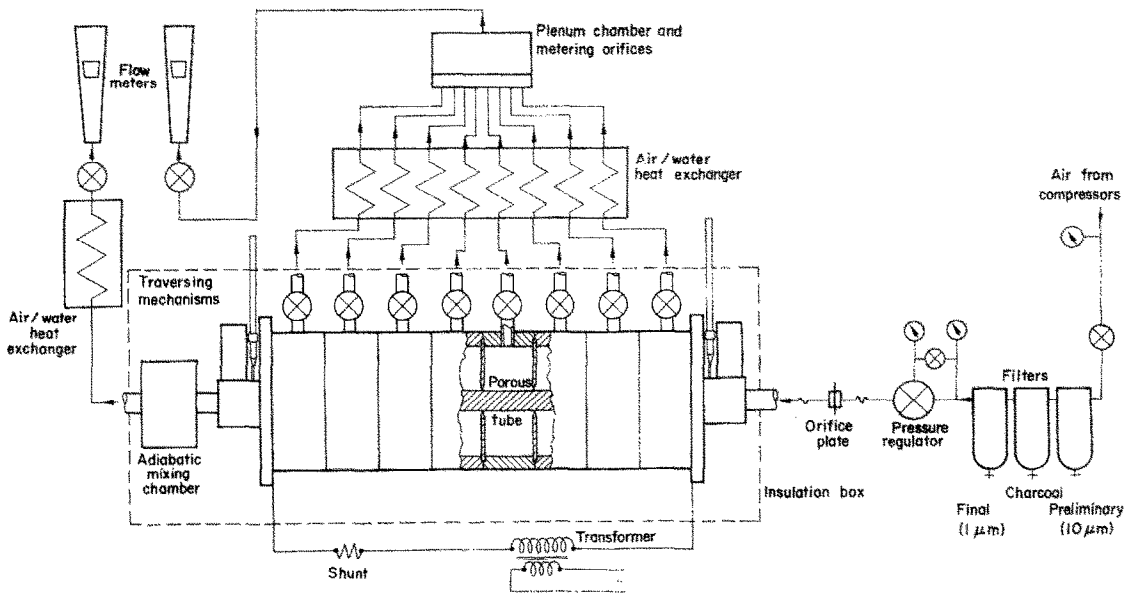

FIG. 2. Schematic representation of apparatus.

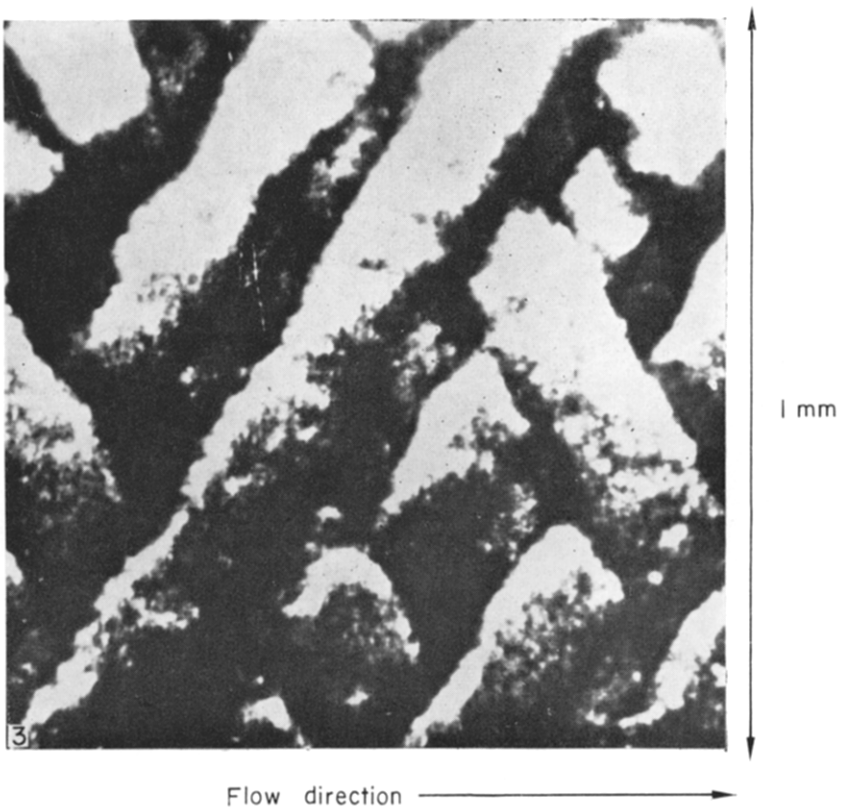

FIG. 3. Surface structure of Poroloy-T.

[*facing page* 596]

mainstream. Stainless steel flanges were vacuum brazed to the ends of the tube and served to carry the electrical heating current into it.

The housing was cylindrical, of about 100 mm i.d., and made of Sindanyo†. (This material is slightly porous and was therefore impregnated with phenolic resin to seal it). It was made up of eight identical cylindrical sections, each section being separated from its neighbours by thin Sindanyo diaphragms, which also fitted closely the outside of the porous tube. By this means the sucked air was divided, along the length of the tube, into eight parts, each part entering a separate chamber formed by the housing and two separating diaphragms. The sucked air was drawn off from each chamber via individual needle valves so that the distribution of sucked air along the tube could be regulated. The eight sucked air flows were then passed through separate water cooled coiled tubes to reduce the flows to a common temperature and then through identical individual orifices so that their relative flow rates could be measured.

Large Sindanyo end flanges located the tube within the housing and carried DISA traversing equipment which allowed thermocouple traverses to be made just ahead of ($x/D = -1$) and just after ($x/D = 21{\cdot}8$) the ends of the porous tube. Provision was made in one of the flanges for the tube to elongate under the effect of heating.

The mainstream air leaving the tube entered an adiabatic mixing chamber, also of Sindanyo, and then passed through a water cooled coiled tube before entering its final control valve and flowmeter.

The porous tube was directly heated by passing an alternating current through it. Heavy cables were used to minimize the circuit resistance but short sections of thinner cable were used for the final connection to the tube flanges, the heat generated in these sections preventing an otherwise large heat loss from the ends of the tube into the heavy cables.

Convective heat losses from the test section were minimized by enclosing it, together with the adiabatic mixing chamber, within a large box filled with expanded vermiculite.

3.3 *Temperature measurements*

Chromel–alumel thermocouples formed from 0·12 mm dia. wire were used for all temperature measurements. These measurements fell mainly into three groups.

(i) Mainstream temperature,
(ii) sucked air temperature, and
(iii) porous tube surface temperature.

Mainstream temperatures were measured at the orifice meter, for the purpose of calculating the flow rate, and by traversing just prior to the porous tube entry. The bulk temperature of the mainstream leaving the tube was measured immediately after the adiabatic mixing chamber and the exit temperature distribution was established by a traverse just beyond the end of the tube. In all cases the velocities were low enough for the effect of dynamic temperature to be neglected.

The sucked air temperature was measured just prior to the needle valve on each of the eight chambers surrounding the tube.

The temperature of the outer surface of the tube was measured by a series of thermocouples spot-welded directly on to the outer surface. Twenty four thermocouples were used in eight sets of three, one set to each chamber. The three junctions in each set were at the same axial location but equispaced around the tube circumference. A further set of three thermocouples was similarly mounted close to the tube entry ($x/D = 0{\cdot}8$). No attempt was made to measure the temperature of the inner surface of the tube.

A number of thermocouples were also embedded within the cables carrying the current to the tube, close to the tube flanges, and these were used to establish the required size of the

† An asbestos cement insulating material manufactured by Turners Asbestos Cement Co. Ltd., Manchester.

thinner 'guard heater' cable sections needed to arrest the heat loss to the cables.

4. REDUCTION OF EXPERIMENTAL DATA †

4.1 *Some general features*

It was not possible to measure the velocity and temperature profiles of the mainstream immediately at entry to the porous tube and so these were obtained at $x/D = -1$. The velocity profile was found to be axisymmetric and hydrodynamically fully developed and the temperature profile was flat (except in the immediate vicinity of the wall). It has been assumed that these were unaltered between $x/D = -1$ and $x/D = 0$ despite surface suction and heat which were applied to the tube discontinuously at $x/D = 0$. In practice, however, there will be some axial conduction of heat from the tube to the Sindanyo end flanges.

The suction rate was made as uniform as possible over the entire tube length. The electric power input was found to be uniformly distributed over the tube length as very little scatter (no greater than $\pm 0{\cdot}5$ per cent) occurred about a least-squares straight line fitted to the measured values of the local voltage.

4.2 *Heat losses*

The sum of the enthalpy rises of the mainstream and the sucked air, Q, was calculated from an energy balance over the entire tube length,

$$Q = m_1 c_p[(1-\alpha)\,t_{b2} - t_{b1} + \alpha\bar{t}_s] \qquad (12)$$

where subscript 2 refers to the outlet of the porous section,
$\alpha = 1 - m_2/m_1$ = fractional mass extraction parameter and the bulk temperature of the sucked air averaged over the whole tube length is

$$\bar{t}_s = \frac{1}{L/D}\int_0^{L/D} t_s \, dx^+. \qquad (13)$$

† Further details of the reduction procedures outlined below may be found in a fuller report by Aggarwal [10].

Q always fell short of the electrical input, Q_i, particularly at low entrance Reynolds numbers and suction rates. The difference was put down to losses occurring by conduction radially through the wall of the housing, any loss from the end flanges having been assumed to be negligible. These losses were assumed to be distributed along the length of the housing in proportion to the temperature difference $(t_s - t_a)$, where t_a is the ambient temperature, so that the local rate of heat loss, per unit x/D, is

$$q_L = A(t_s - t_a) \qquad (14)$$

and the local rate of heat transfer to the air per unit x/D is

$$q = \frac{Q_i}{L/D} - q_L. \qquad (15)$$

The constant of proportionality, A, was established from the known value of the overall heat loss $(Q_i - Q)$.

4.3 *Temperature distributions*

Both the sucked air temperature, t_s, and the tube outer surface temperature, t_{out}, were found to exhibit some scatter, but in both cases least-squares second order curves gave a very satisfactory fit (typical standard deviation was 0·004) to the experimental points and values read from these curves were used in all subsequent calculations.

The temperature of the inner surface of the porous tube, t_w, was computed from a knowledge of the outer surface temperature by integrating the appropriate energy equation for the wall

$$\frac{1}{r}\frac{\partial}{\partial r}\left(r\frac{\partial t}{\partial r}\right) + \frac{\partial^2 t}{\partial x^2} + \frac{q_g}{k_p} = 0 \qquad (16)$$

where q_g is the rate of heat generated per unit volume $(= Q_i/\pi DLw, w =$ thickness of the porous wall) and k_p is the thermal conductivity of the porous material. Strictly speaking, this analysis applies only to the case of no-suction. However, as the amount of heat picked up by the sucked air within the interstices of the porous wall, Q_s,

was found to be only a small fraction (typically 0·5 per cent) of the electrical heat generated, little error was introduced in assuming that Q_s was uniformly distributed throughout the wall so that q_g in equation (16) could be replaced by $(Q_i - Q_s)/\pi DLw$ to enable t_w to be determined in the presence of suction.

The local bulk temperature of the mainstream, t_b, which could not be measured by experiment, was evaluated by integration of the energy equation applied to the control volume EFGH of Fig. 1,

$$q = \frac{\mathrm{d}}{\mathrm{d}x^+}(mc_p t_b) + 4m_1\beta_1 c_p t_s \qquad (17)$$

both q and t_s having already been determined.

4.4 *Apparent Nusselt number with suction*

Having established the bulk temperature variation of the mainstream, the local apparent Nusselt number, Nu_{Da}, was calculated from equation (6). The average apparent Nusselt number $\overline{Nu_{Da}}$ over the tube length x is given by

$$\overline{Nu_{Da}} = \bar{h}_a \frac{D}{k} = \frac{m_1 c_p (t_b - t_{b1})}{\pi D k x^+ \overline{\Delta t}} \qquad (18)$$

where $\overline{\Delta t}$ was evaluated with the aid of equation (11).

Values of $\overline{Nu_{Da}}$ were computed over various tube lengths up to $x/D = 20{\cdot}8$. At $x/D = 0$, equation (18) becomes indeterminate, but it is clear that at the entry section the average value coincides with the local value of the apparent Nusselt number as calculated from equation (6).

4.5 *Actual Nusselt number with suction*

It was pointed out elsewhere that the computation of Nu_D requires a knowledge of the sucked air temperature at entry to the porous wall, t_{sw}. The latter has been established on the basis of an approximate figure for the interstitial heat transfer coefficient, h_i, obtained from the experimental data of Bayley and Turner [9].

The interstitial heat transfer rate per unit x/D within the porous material, q_s, is governed by the equation

$$q_s = h_i \pi D^2 w[t_{out} - \tfrac{1}{2}(t_{sw} + t_s)] \qquad (19)$$

if the radial gradient of metal temperature within the wall is ignored. This heat transfer gives rise to an increase in the temperature of the sucked air from t_{sw} to t_s so that

$$q_s = 4m_1\beta_1 c_p(t_s - t_{sw}). \qquad (20)$$

Combining equations (19) and (20), one obtains

$$t_{sw} = t_s - \frac{2B}{1 - B}(t_{out} - t_s) \qquad (21)$$

where

$$B = \frac{h_i}{4m_1\beta_1} \cdot \frac{\pi D^2 w}{2c_p}. \qquad (22)$$

The data of Bayley and Turner [9] suggest that h_i is a linear function of the mass flow $(4m_1\beta_1)$ through the porous material. For the case of uniform suction, therefore, B is a constant and its value was equal to 0·0408 in the present experiments. Having established t_{sw}, Nusselt number with suction followed from equation (8).

The average Nusselt number with suction up to a given location in the tube is defined by

$$\overline{Nu_D} = \frac{\int_0^{x^+} q_m \,\mathrm{d}x^+}{\pi D k x^+ \overline{\Delta t}}. \qquad (23)$$

Note that

$$\overline{Nu_D} \neq \frac{1}{x^+}\int_0^{x^+} Nu_D \,\mathrm{d}x^+$$ because the temperature difference $\overline{\Delta t}$ is not defined as

$$\int_0^{x^+} (t_w - t_b)\,\mathrm{d}x^+ \qquad \text{(see equation 11).}$$

By substituting for the first term on the R.H.S. of equation (21) from equation (2), one obtains

$$q_m = q - 4m_1\beta_1 c_p(t_s - t_{sw}) \qquad (24)$$

and thus $\overline{Nu_D}$ follows from the previously established quantities q, t_s and t_{sw}.

5. RESULTS

5.1 *General*

Tests were carried out at four values of the inlet Reynolds number, Re_{D1}, 9930, 19760, 50550, 102350. Results with suction reported here are for only two of these values, generally 19760 and 102350, since these were found to demonstrate the effects of inlet Reynolds number sufficiently clearly.

The apparatus was first used to establish heat transfer coefficients without suction in order both to prove the rig and to provide base values for the subsequent results with suction. The electrical power input was kept constant at all suction rates for a given inlet Reynolds number. The former ranged from about 50 W at the lowest Reynolds number to about 500 W at the highest. The total heat loss from the test section was generally small, but at the lowest value of Re_{D1} it was as high as 20 per cent of Q_i for 10 per cent suction. The loss, however, fell sharply as both suction rate and Reynolds number increased, and for $\alpha > 0{\cdot}3$ the loss was negligible at all the higher Reynolds numbers.

5.2 *Nusselt number without suction*

For all the values of Re_{D1} the no-suction Nusselt number, Nu_{D0}, was found to fall with x/D, reach a minimum value around $x/D = 15$, and then rise somewhat. This rise in Nu_{D0} beyond the point at which the temperature profile had probably become fairly well established was attributed to heat losses from the end of the tube. The computation for the heat supplied to the air per unit length, and thus for the rate of rise of mainstream bulk temperature, was based upon the assumption that the entire loss occurred radially, and as a result of this the computed heat flux to the mainstream was almost constant. However, the existence of a finite end loss meant that in practice the heat flux to the mainstream, and hence the bulk temperature, were overestimated near the exit of the tube, thus giving rise to apparently high Nusselt numbers in this region. A similar effect occurred near the entrance to the tube but the large gradients of surface temperature in this region masked any influence upon Nusselt number.

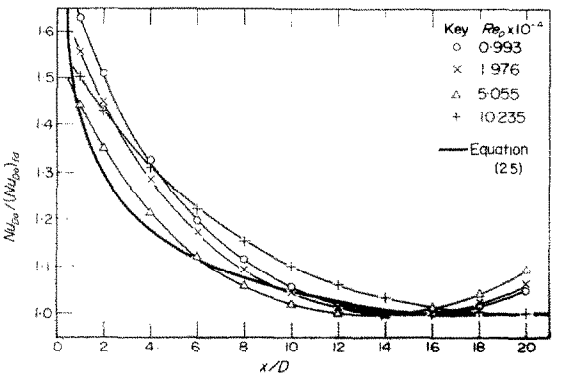

FIG. 4. No-suction Nusselt numbers along the tube.

The minimum value of Nu_{D0} was therefore taken as that corresponding to a fully developed temperature profile, and it was used to normalise the local values, the results being shown in Fig. 4. These Nusselt numbers are based upon property values at the mean bulk temperature. Also plotted in Fig. 4 is an empirical curve [11] for a hydrodynamically smooth tube under similar flow conditions, based upon experimental data of many previous workers, and which is independent of Reynolds number,

$$\frac{Nu_{D0}}{(Nu_{D0})_{fd}} = \frac{1}{0{\cdot}693 + 0{\cdot}26 \log_{10} x^+} \quad \text{for } 0{\cdot}022 < x^+ < 15, \qquad (25)$$

$$= 1 \quad \text{for } x^+ \geqslant 15.$$

The experimental curves for the porous tube are generally of the same order, the somewhat larger values probably being attributable to the roughness of the tube. A further reason for the differences may be that, despite there having been no net suction, some circulation will inevitably have taken place within the chambers surrounding the tube, giving rise to variations in the local velocity and heating patterns close to the inner surface.

The values for $(Nu_{D0})_{fd}$ were modified to give

'constant property' values $(Nu_{DO})_{fd,c}$ using

$$(Nu_{DO})_{fd\ c} = (Nu_{DO})_{fd} \times \left(\frac{t_w}{t_b}\right)^{0.45} \quad (26)$$

and these are shown in Fig. 5. They lie on the line

$$(Nu_{DO})_{fd,c} = 0.019\, Re_D^{0.8} \quad (27)$$

which compares well with the relation for smooth tubes, an approximation to the empirical correlation in [8],

$$(Nu_{DO})_{fd,c} = 0.0178\, Re_D^{0.8} \quad (28)$$

Where experimental no-suction Nusselt numbers have been used as base values with which to compare Nusselt numbers with suction they are based on property values at mean bulk temperature, since the effect of varying properties under suction conditions is unknown.

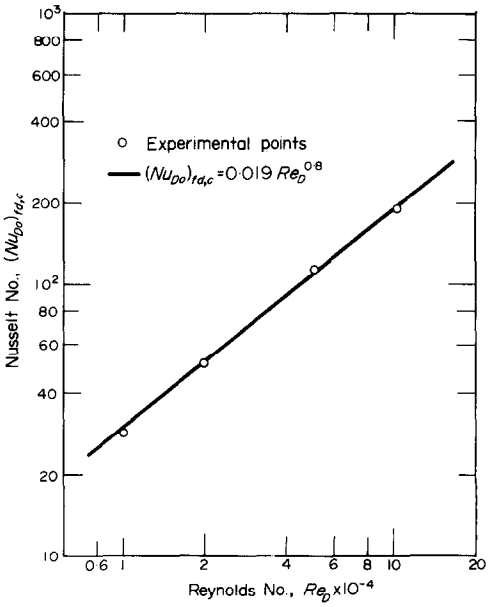

FIG. 5. Fully-developed, no-suction Nusselt numbers.

5.3 *Radial temperature profiles*

Radial temperature profiles taken one diameter beyond the exit of the tube for a range of suction rates and an inlet Reynolds number of 102 350 are depicted in Fig. 6, in which t_i is the temperature recorded by the traversing thermocouple when touching the wall, which in this case was the surface of the bore in the Sindanyo flange. Since this was considerably lower than the temperature of the inner surface at the exit of the porous tube, the numerical values should be treated with caution. Nonetheless the relative shapes of the profiles may be compared with confidence.

Increasing the suction rate is seen to have the effect of steepening the temperature profile close to the surface and so increasing the rate of heat transfer from it. However, at high rates of suction little of this heat is retained by the mainstream since a substantial part of it is removed with the sucked air. Consequently the temperature profile becomes quite flat, save in the vicinity of the wall, and the bulk temperature of the mainstream rises only slowly with distance from the tube entrance (see section 5.4). Although the profiles at high rates of suction resemble those occurring in the thermal entrance region

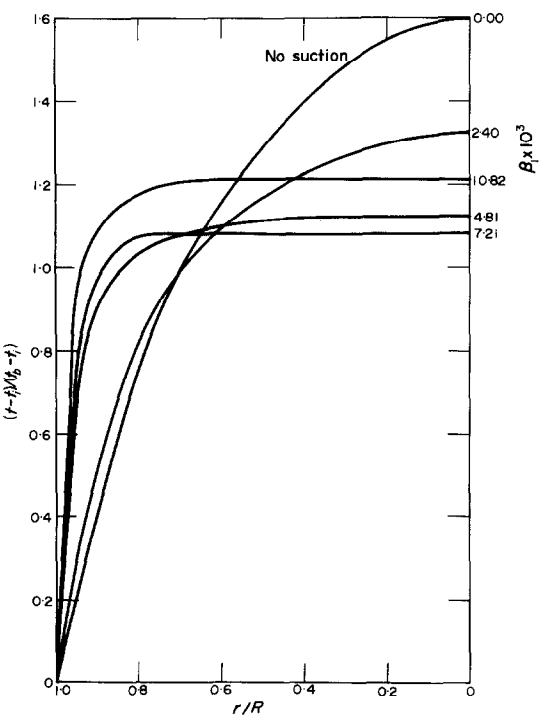

FIG. 6. Non-dimensional temperature profiles, Re_{D1} = 102 350.

of an impervious tube, the situation is slightly different since the centreline temperature was found to rise over the tube length, the enhanced turbulence due to suction [1, 10] probably giving rise to a heat transfer across the core.

5.4 *Bulk temperature of the mainstream*

Figure 7 shows the variation along the tube of the non-dimensional bulk temperature of the mainstream for an inlet Reynolds number of 102 350 and a range of suction rates. The temperature rise along the tube has been non-dimensionalized using the rate of supply of heat, Q/m_1c_p. [The largest bulk temperature rise recorded over the test section was about 18 K (no suction) and the lowest reliable value about 2 K (90 per cent suction).]

The bulk temperature rise is seen to be consistently reduced as the rate of suction is increased, and it is clear that at high rates of suction, only a very small proportion of the total heat lost from the inner surface is retained by the mainstream. At lower values of Re_{D1} a greater proportion is retained.

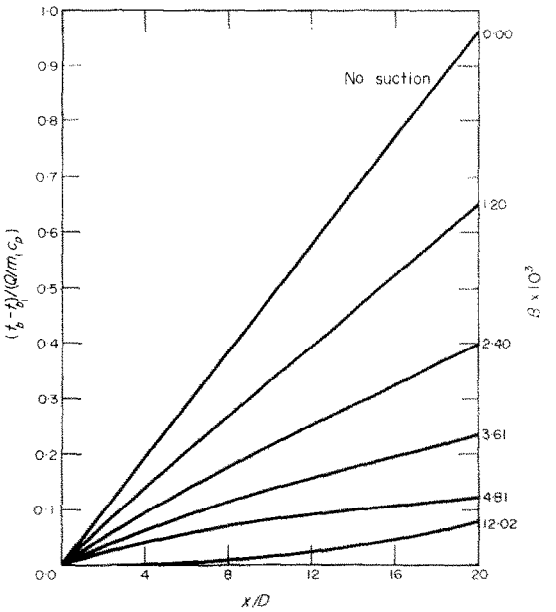

FIG. 7. Non-dimensional bulk temperature of mainstream $Re_{D1} = 102\,350$.

5.5 *Inner surface temperature*

The variation along the tube of the normalized inner surface temperature, computed from the measured outer surface temperature, is depicted in Fig. 8 for various suction rates and an inlet Reynolds number of 102 350. As with the mainstream bulk temperature, the rate of rise of surface temperature falls steadily with increasing suction so that for $\beta_1 > 9{\cdot}62 \times 10^{-3}$ scarcely any discernible rise in temperature occurs. The results at the lower values of Re_{D1} were similar save that at the lowest value ($Re_{D1} = 9930$) coupled with the lowest suction rate ($\beta_1 = 1{\cdot}20 \times 10^{-3}$), the normalized wall temperature rise appeared to be greater than that for no suction. Since this was the condition under which the percentage heat loss was largest too much should not be read into this, although there is clearly scope for a more detailed investigation at these low rates of suction.

An interesting feature, not revealed by these

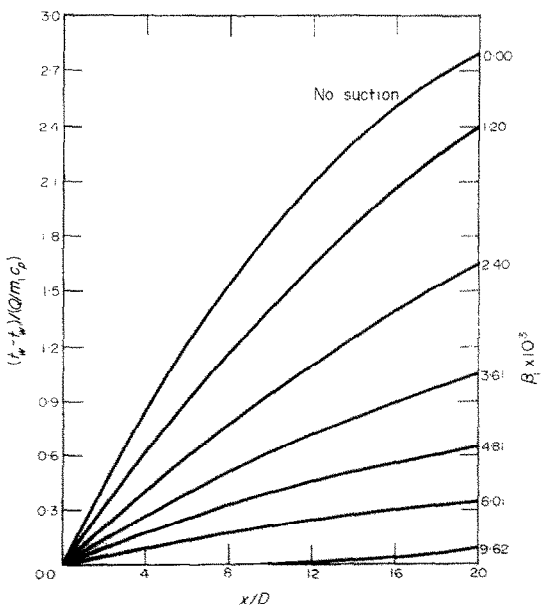

FIG. 8. Non-dimensional wall temperature $Re_{D1} = 102\,350$.

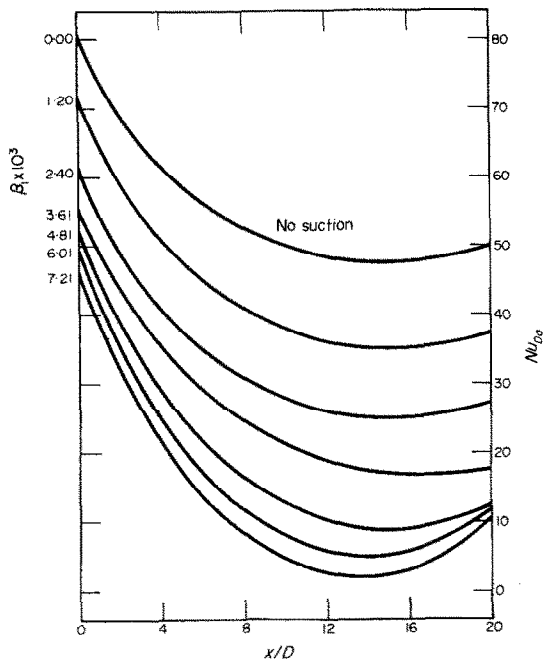

FIG. 9. Local apparent Nusselt number, $Re_{D1} = 19\,760$.

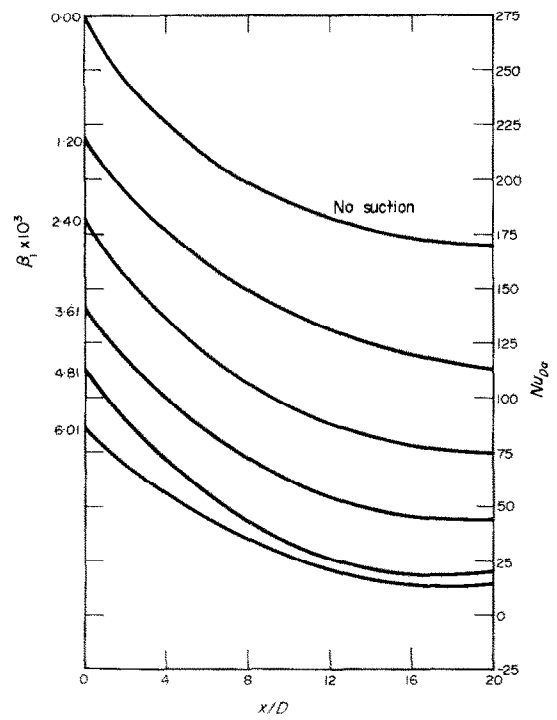

FIG. 10. Local apparent Nusselt number, $Re_{D1} = 102\,350$.

non-dimensionalized curves, is that not only was the rate of rise of surface temperature, per unit heat supplied, generally lowered by suction but the temperature itself (never greater than 131°C), for a fixed Q, m_1, t_{b1} and x/D, was also lowered. This wall cooling effect was particularly marked in the region of the tube exit at low rates of suction and at high inlet Reynolds numbers.

5.6 *Apparent Nusselt number*

Local apparent Nusselt numbers, Nu_{Da}, as defined by equation (6) are displayed for inlet Reynolds numbers of 19 760 and 102 350 in Figs. 9 and 10 respectively. As expected from the previously described temperature distributions, the local apparent Nusselt number, compared with the corresponding no-suction value, falls as suction is applied. At high rates of suction the results suffer from inaccuracy, particularly at the higher entrance Reynolds numbers, since very small rises in t_b were observed and under these conditions a small error in this measurement can introduce large errors in Nu_{Da}. Hence results for high suction rates have been omitted from these figures. At low rates of suction the rise of Nu_{Da} towards the tube exit (mentioned in section 5.2 in the context of no-suction Nusselt number) is apparent at the lower inlet Reynolds numbers.

Average apparent Nusselt numbers, $\overline{Nu_{Da}}$, are given as a 'carpet' plot in Fig. 11 for $Re_{D1} = 19\,760$, where β_1 and x/D are the two floating variables. The curves clearly follow the pattern exhibited by the local values, with the same shortcomings at high rates of suction, the curves for $\beta_1 > 6{\cdot}01 \times 10^{-3}$ probably not being very accurate. At the higher Reynolds numbers, at least for low rates of suction, similar curves are obtained and in order to quantify the effect of Reynolds number a correlation of the form

$$\overline{Nu_{Da}} = P \times Re_{D1}^{p} \qquad (29)$$

where both P and p are functions of β_1 and x/D, was sought. For suction rates up to $\beta_1 = 3{\cdot}61 \times 10^{-3}$ clearly defined values of p depending upon both β_1 and x/D, could be established.

Curves depicting p vs. β_1 are shown in Fig. 12 for a range of values of x/D. For the case of no-suction p is seen to approach 0·8 at large x/D, but as suction increases the dependence upon Re_{D1} falls, the fall being particularly marked at $x/D = 20$. Calculations for $\overline{Nu_{Da}}$ at higher Reynolds numbers based on data from Figs. 11 and 12 gave values within 5 per cent of the experimentally determined figures in the range $\beta_1 = 0$ to $\beta_1 = 3{\cdot}61 \times 10^{-3}$.

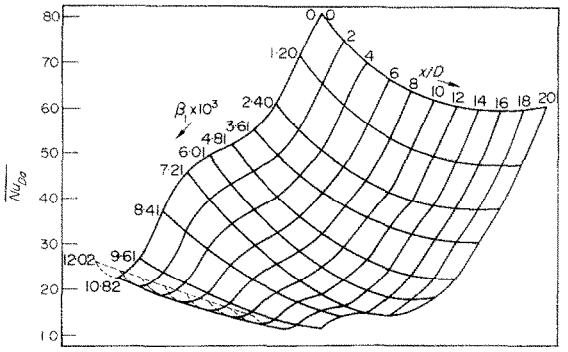

FIG. 11. Average apparent Nusselt number, $Re_{D1} = 19\,760$.

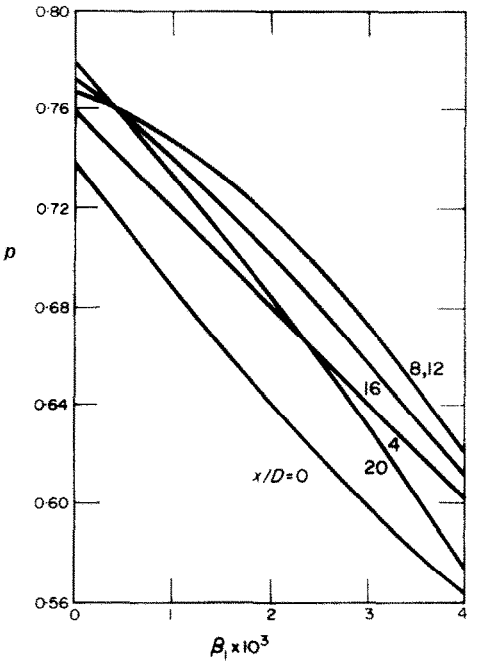

FIG. 12. Exponent of inlet Reynolds number for $\overline{Nu}_{Da}$.

5.7 *Nusselt number*

The value of the local Nusselt number, computed with the aid of interstitial heat transfer data [9], has been divided by the constant property, no-suction, Nusselt number given by

$$Nu_{D0,c} = \frac{0{\cdot}019\,Re_D^{0{\cdot}8}}{0{\cdot}693 + 0{\cdot}26\log_{10} x^+} \quad \text{for } 0{\cdot}022 < x^+ < 15$$

$$= 0{\cdot}019\,Re_D^{0{\cdot}8} \quad \text{for } x^+ \geqslant 15$$

and the results are presented for $Re_{D1} = 19\,760$ and 102 350 in Figs. 13 and 14. The Nusselt numbers, particularly at large suction rates and large x/D, are seen to be appreciably greater than the corresponding no-suction values at the same local Reynolds numbers. These enhanced Nusselt numbers follow from the large temperature gradients in the air near the inner surface (section 5.3), gradients which increase

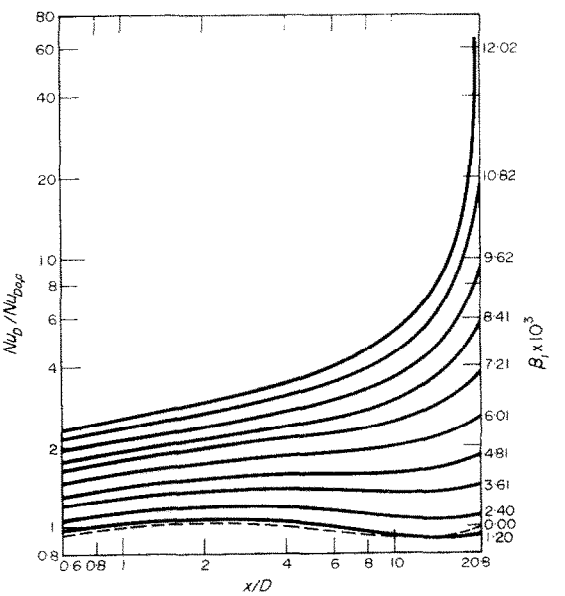

FIG. 13. Local Nusselt number, $Re_{D1} = 19\,760$ (based on data for h_i from [9]).

with suction rate in line with the increase in Nusselt number seen in these figures. Similar results were obtained at the other inlet Reynolds numbers.

The dotted curves in these figures are for no-suction, and they show the deviation of the experimental values from the empirical curve already discussed in section 5.2, together with a very small difference due to the 'constant property' form of the latter. This deviation is also apparent in the curves for low suction rates, but as the suction rate increases any such differences are overridden by the large effects of suction.

Nusselt numbers averaged up to a range of values of x/D are shown in Fig. 15 as a 'carpet plot'. The inlet Reynolds number for the figure is 102 350. The effect of suction is large, giving rise to enhanced Nusselt numbers at all rates of suction. Note that at high rates of suction, at least at this Reynolds number, $\overline{Nu_D}$ appears to be almost independent of x/D, suggesting that under these conditions hardly any growth in the thermal boundary layer occurs along the tube.

A correlation of the average Nusselt number (for air only) in terms of inlet Reynolds number, inlet suction coefficient and length/diameter ratio of the form

$$\overline{Nu_D} \propto Re_{D1}^{n} \beta_1^{d} (x/D)^{b} \tag{30}$$

was sought by logarithmic plotting. Both a and b appear to be dependent upon all three variables, and so cannot be clearly defined, but log $\overline{Nu_D}$ vs. log Re_{D1} yields, for fixed values of β_1 and x/D, straight lines with virtually no scatter. The slope of these lines, n, increases consistently with both β_1 and x/D, and the dependence of n upon these variables is depicted in Fig. 16. Trial calculations for $\overline{Nu_D}$ for a range of Re_{D1}, β_1 and x/D using the relation

$$\overline{Nu_D} = N \times Re_{D1}^{n} \tag{31}$$

where N is a function of β_1 and x/D, have been made using the data from Figs. 15 and 16, and in all cases the calculated values are within 5 per cent of the experimentally determined

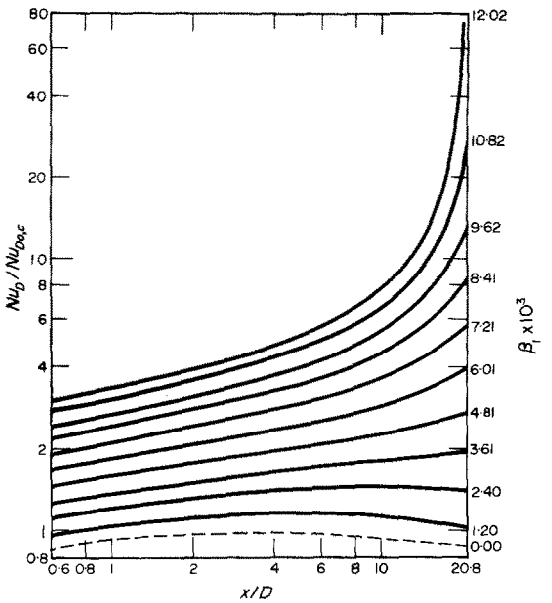

FIG. 14. Local Nusselt number, $Re_{D1} = 102\,350$ (based on data for h_i from [9]).

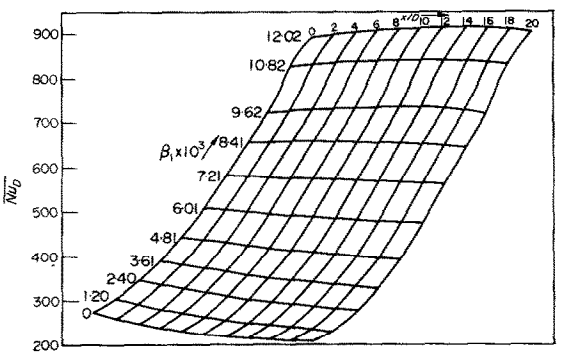

FIG. 15. Average Nusselt number with suction, $Re_{D1} = 102\,350$ (based on data for h_i from [9]).

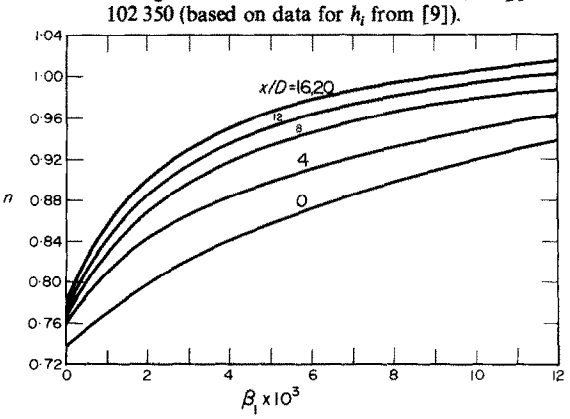

FIG. 16. Exponent of inlet Reynolds number for $\overline{Nu_D}$.

results, so that these figures may be used with confidence for predicting average Nusselt numbers in the range $10^4 < Re_{D1} < 10^5$.

Both the local and the average Nusselt numbers depend upon the value used for the interstitial heat transfer coefficient, h_i, and the only data available for Poroloy were for flat sheets where the air entered and left the plate normally, a condition probably different from that occurring in a tube. However, since the tube used in the present experiments had a very thin wall, q_s was only a small fraction of q_m, with the result that large changes in h_i had little effect upon the calculated Nusselt numbers.

5.8 *Comparison with other results*

To the best of the authors' knowledge the only other data on heat transfer in porous tubes with turbulent flow is that from the theoretical work of Kinney and Sparrow [7]. Their temperature profiles resemble very closely in form those depicted in Fig. 6, but since their theory required the assumption of self-similar temperature (and velocity) profiles their Nusselt numbers were independent of x/D. Nevertheless, a comparison has been attempted in Fig. 17 where their results, in the form of a ratio of Nusselt number with suction to Nusselt number without, have been plotted against local suction rate, β, for local Reynolds numbers of 10 000 and 50 000 and compared with experimental values at $x/D = 16$ for four inlet Reynolds numbers. Although this comparison is not really valid, since the local Reynolds number for the experimental curves varies with β, it shows that the order of magnitude of Kinney and Sparrow's values is similar to that of the experimental results.

Turning now to the heat transfer coefficients, Bayley and Turner [4] took the value of the heat transfer coefficient for their blade passages, as a first estimate, to be that pertaining to fully developed turbulent flow, h_{fd}, at the locally prevailing Reynolds number. Furthermore, since no information was hitherto available concerning the temperature, t_{sw}, at which the sucked air entered the porous wall, it was

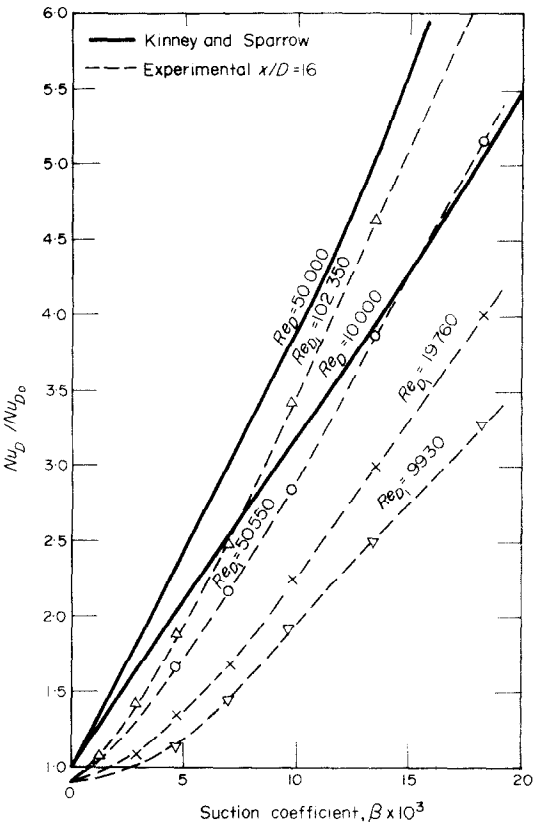

FIG. 17. Local Nusselt number.

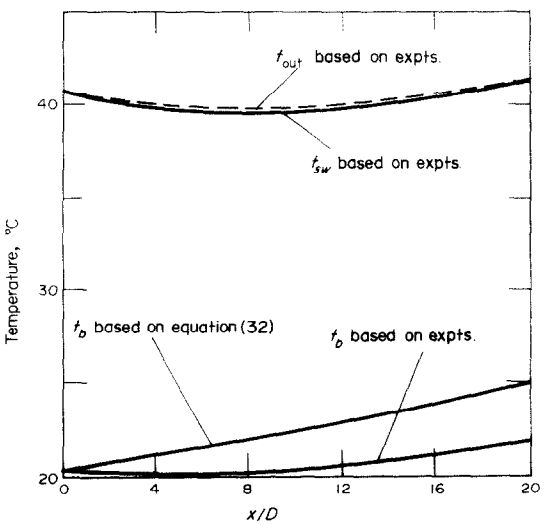

FIG. 18. Wall, bulk and sucked air temperatures, $Re_{D1} = 102\,350$, $\beta_1 = 12{\cdot}02 \times 10^{-3}$

assumed to enter at the bulk temperature, t_b. Under these conditions the rate of rise, along the tube, of the bulk temperature is governed by

$$m_1(1 - 4\beta_1 x^+)\, c_p \frac{dt_b}{dx^+} = \pi D^2 h_{fd}(t_w - t_b). \quad (32)$$

Values for t_b based on this equation are shown in Fig. 18 for a typical case of 100 per cent suction at $Re_{D1} = 102\,350$, using the appropriate experimental value for t_{b1} (20·25°C) and assuming a constant wall temperature of 39°C (which is seen to be closely adhered to in the experiment), with

$$h_{fd} = 0{\cdot}023 \frac{k}{D} Re_D^{0{\cdot}8} Pr^{0{\cdot}4}. \quad (33)$$

Equations (32) and (33) are seen to *overestimate* the bulk temperature of the air but grossly *underestimate* the temperature at which the air enters the porous wall (assumed equal to t_b in the calculation) and therefore underestimate the total quantity of heat that can be transferred to the mainstream. This was why the anticipated blade tip temperatures were lower than those determined experimentally by Bayley and Turner.

6. CONCLUSIONS

Measurements of axial wall temperature distribution were obtained on a 'Poroloy' tube carrying an initially hydrodynamically fully-developed turbulent flow of air subjected to uniform surface suction. The tube was electrically heated. The sucked air temperature and the voltage along the tube were also measured. The bulk temperature of the mainstream was computed from the measured temperatures with the aid of the energy equation for a range of entrance suction coefficient, β_1. These in turn led to the evaluation of local and average apparent Nusselt numbers as functions of a suction parameter and of location along the tube. The local and average values of the actual Nusselt number with suction were calculated using values for the interstitial heat transfer coefficient given by Bayley and Turner [9].

1. For fixed entry conditions, and for a given amount of heat input, the wall temperature is lowered by increasing suction. Save possibly at very low values of β_1, the effect of increased suction is to make the rate of wall temperature rise along the tube smaller, and this reduction is more pronounced at higher inlet Reynolds numbers.
2. The bulk temperature of the mainstream rises less rapidly along the tube with suction than without.
3. The application of suction steepens the temperature profile in the wall region and flattens it in the core implying that the thermal boundary layer grows more slowly with suction.
4. The local and average apparent Nusselt numbers with suction decrease with both β_1 and x/D. Nu_{Dx} and $\overline{Nu_{Dx}}$ are higher for larger values of Re_{D1}, and for low rates of suction $\overline{Nu_{Dx}}$ is of the form $P \times Re_{D1}{}^p$ where both P and p are functions of β_1 and x/D.
5. The Nusselt number with suction is greater than the corresponding Nusselt number without suction, substantially so at large values of x/D. This increase becomes greater with β_1 and Re_{D1}, such that for 100 per cent suction, $Nu_D/Nu_{D0,c}$ half way along the tube tested ranged from 4 at $Re_{D1} \simeq 10^4$ to 8 at $Re_{D1} \simeq 10^5$.
6. The average Nusselt number, $\overline{Nu_D}$, up to any x/D location increases with both β_1 and Re_{D1} but decreases with x/D. For all rates of suction, $\overline{Nu_D} = N \times Re_{D1}{}^n$ where both N and n are functions of β_1 and x/D.

In short, whereas the actual Nusselt number is much higher with suction than without, the bulk temperature of the mainstream does not rise as rapidly because much of the heat input to the latter is being drawn off with the air sucked through the wall.

ACKNOWLEDGEMENT

The authors are indebted to the Bristol Engine Division of Rolls-Royce (1971) Ltd. for their financial support during this research programme.

REFERENCES

1. J. K. AGGARWAL, M. A. HOLLINGSWORTH and Y. R.

MAYHEW, Experimental friction factors for turbulent flow with suction in a porous tube, *Int. J. Heat Mass Transfer* **15**, 1585–1602 (1972).
2. F. J. BAYLEY and A. B. TURNER, Transpiration cooled turbines, *Proc. Instn Mech. Engrs* **185**, 943–951 (1970).
3. F. J. BAYLEY and A. B. TURNER, The transpiration-cooled gas turbine, The University of Sussex, Report No. 69/ME/13 (1969).
4. F. J. BAYLEY and A. B. TURNER, The heat transfer performance of porous gas turbine blades, *Aeronaut. J.* **72**, 1087–1094 (1968).
5. J. P. EDWARDS, Transpiration-cooled cascade tests at NGTE, ARC 31528, HMT 231 (Nov. 1969).
6. J. P. EDWARDS, Summary of Curtiss Wright publication on transpiration cooling, ARC 31529, HMT 232 (Nov. 1969).
7. R. B. KINNEY and E. M. SPARROW, Turbulent flow, heat transfer, and mass transfer in a tube with surface suction, *Trans. Am. Soc. Mech. Engrs* **92C**, 117–125 (1970).
8. I. Chem. E. and I. Mech. E. Forced convection heat transfer in circular tubes—Part I, Engineering Sciences Data Item No. 67016 (April 1967).
9. F. J. BAYLEY and A. B. TURNER, Private communication.
10. J. K. AGGARWAL, Skin friction and heat transfer for turbulent flow with suction in porous tubes, Ph.D. thesis, University of Bristol (1971).
11. I. Chem. E. and I. Mech. E. Forced convection heat transfer in circular tubes—Part III, Engineering Sciences Data Item No. 68007 (August 1968).

TRANSFERT THERMIQUE POUR UN ECOULEMENT TURBULENT DANS UN TUBE POREUX AVEC SUCCION

Résumé—Des mesures de la distribution axiale de température superficielle ont été obtenues sur un tube poreux siège d'un écoulement d'air et soumis à un chauffage électrique uniforme. Il existait à l'entrée du tube un écoulement turbulent entièrement développé hydrodynamiquement et l'extraction massique à travers la paroi était uniforme. La température moyenne locale de l'écoulement principal a été évaluée à l'aide de l'équation d'énergie. Les expériences ont couvert un domaine du nombre de Reynolds d'entrée compris entre 10^4 et 10^5 avec un rapport vitesse transversale en paroi/vitesse axiale principale à l'entrée de 0 à environ 0,02 (c'est-à-dire depuis l'absence de succion jusqu'à cent pour cent de la succion). La distribution radiale de température mesurée dans le plan de sortie du tube indique que la forme du profil de température est sensible à la succion, devenant plus pentu près de la paroi et plus plat près de l'axe du tube. Des valeurs aussi bien locales que moyennes du nombre de Nusselt avec succion ont été calculées et présentées sous forme graphique. Pour un nombre de Reynolds fixé à l'entrée, ces valeurs augmentent nettement avec la succion et diminuent avec x/D bien que les valeurs locales homologues en l'absence de succion augmentent le long du tube. On présente aussi une relation empirique pour le nombre de Nusselt moyen. Afin de décrire le débit de chaleur fournie à l'air restant dans le tube, par opposition au débit total de chaleur comprenant la chaleur fournie à l'air aspiré avant qu'il ne pénètre la paroi poreuse, on a considéré un nombre "apparent" de Nusselt et les nombres apparents de Nusselt locaux et moyens diminuent alors que la succion et x/D diminuent.

WÄRMEÜBERGANG IN EINEM PORÖSEN ROHR BEI TURBULENTER STRÖMUNG

Zusammenfassung—Es wurden Messungen durchgeführt über die axiale Oberflächentemperaturverteilung in einem porösen Rohr, bei Strömung von Luft und einheitlicher elektrischer Beheizung. Hydrodynamisch voll entwickelte turbulente Strömung herrschte am Rohreintritt, der Massenaustritt durch die Wand war einheitlich. Die örtliche Stautemperatur des Hauptstromes wurde mit Hilfe der Energiegleichung gefunden. Die Experimente überdeckten eine Eingangs-Reynolds-Zahl von 10^4 bis 10^5 mit einem Verhältnis der Quergeschwindigkeit an der Wand zur Hauptaxialgeschwindigkeit am Eingang von 0 bis ungefähr 0,012 (d.h. von Ansaugung Null bis 100%). Die gemessene radiale Temperaturverteilung in der Austrittsebene des Rohres zeigt, dass die Form des Temperaturprofils markant durch das Saugen beeinflusst wird, indem es steiler nahe der Wand wird und flacher zur Rohrachse hin. Sowohl örtliche als auch durchschnittliche Werte der Nusselt-Zahl mit Ansaugung wurden berechnet und graphisch aufgetragen. Bei einer bestimmten Eingangs-Reynolds-Zahl stiegen diese beiden Werte mit Absaugung an und fielen mit x/D ab, obwohl die örtlichen Werte relativ zu ihren Gegenstücken ohne Absaugung entlang des Rohres abfielen. Eine empirische Beziehung für die durchschnittliche Nusselt-Zahl mit Saugen wird ebenfalls gegeben. Zur Bestimmung des Verhältnisses aus dem Wärmebedarf der im Rohr verbleibenden Luft und des gesamten Wärmebedarfs, einschliesslich der Lufterwärmung vor Eintritt in die poröse Wand wurde eine "scheinbare" Nusselt-Zahl eingeführt. Sowohl die örtliche wie auch die durchschnittliche Nusselt-Zahl fiel mit ansteigender Absaugung und steigendem x/D ab.

ТЕПЛООБМЕН В ТУРБУЛЕНТНОМ ПОТОКЕ В ОТСОСОМ В ПОРИСТОЙ ТРУБЕ

Аннотация—Измерялось аксиальное распределение температуры по поверхности пористой трубы, равномерно нагреваемой электричеством, при течении в ней воздуха. На входном участке трубы существовал полностью развитый турбулентный поток. Через стенку трубы осуществлялся однородный отсос массы. С помощью уравнения энергии определялась среднеобъёмная температура в различных сечениях. В экспериментах охвачен диапазон чисел Рейнольдса на входе от 10^4 до 10^5 при отношении поперечной скорости на стенке к средней продольной скорости на входе от нуля до, примерно, 0,012 (т.е. от случая отсутствия отсоса до случая 100%-го отсоса). Радиальное распределение температуры, измеренное в плоскости выхода трубы, указывает на то, что температурный профиль претерпевает значительные изменения благодаря отсосу, становясь более крутым у стенки и более пологим у оси трубы. Подсчитаны и представлены графически локальные, а также средние значения числа Нуссельта при отсосе. При фиксированном числе Рейнольдса на входе оба эти значения увеличиваются при отсосе и уменьшаются с отношением x/D, хотя локальные значения при отсутствии отсоса увеличиваются вдоль трубы. Представлено также эмпирическое соотношение для среднего числа Нуссельта при отсосе. Для описания интенсивности подвода тепла к остающемуся в трубе воздуху в противоположность общему подводу тепла, включающему тепло, подводимое к отсосанному воздуху, прежде чем он поступит в пористую стенку, вводилось «мнимое» число Нуссельта. Как локальное, так и среднее мнимые числа Нуссельта уменьшались с увеличением отсоса и отношения x/D.